Journal of Engineering Sciences, Assiut University, Vol. 35, No. 4, pp. 957-973, July 2007

NET EFFECTIVE GAIN OF MULTI-PUMPING RAMAN AMPLIFIER IN ULTRA-WAVELENGTH DIVISION MULTIPLEXING AND ULTRA-LONG – HAUL OPTICAL COMMUNICATION SYSTEMS

Abd El-Naser A. Mohammed

Department of Electronic and Electrical Communication Engineering, Faculty of Electronics Engineering (FEE), Menouf, 32951, Minufiya University, EGYPT
Email: abd_elnaser6@yahoo.com

(Received February 26, 2007 Accepted June 30, 2007)

In the present paper, a net effective gain of multi-pumping Raman amplifier in ultra-wavelength division multiplexing (UW-WDM) and ultra long-haul (ULH) optical communication systems has been modeled and parametrically investigated over wide ranges of affecting parameters, taking into account the polarization effect. NR pumps are processed with or without equal spectral spacing. The effective fiber core area, the gain coefficients and the amplified spontaneous emission power ASE (as a measure of the minimum detectable power) are calculated over the operating wavelength. The above three quantities are cast in simple polynomial forms. The average net Raman gain, the on-off Raman gain, the signal-to-noise ratio at the effective length has been investigated also. The obtained results are employed to find the average repeater spacing over the spectral range under the processing. It is concluded that for repeater spacing, the total injected Raman powers are the vital factor rather than the number of amplifiers, while for the gain spectral width, the number of amplifiers is the vital factor. The central wavelength of the subset of channels that propagates in a link indicates the order of link. The total number of links in the core determines the ultimate values of different effects.

KEYWORDS: *Multi-Pumping Raman Amplifiers, Ultra-Long Haul Optical Communication Systems, Ultra-Wide Wavelength Division Multiplexing*

I. INTRODUCTION

Fiber Raman amplification using transmission line is a promising technology to increase the repeater distance as well as the capacity of the communication systems. Because of the growing importance of fiber Raman amplification, it is desired to predict the magnitude and shape of the Raman gain spectrum from the doping level and refractive index profiles of different fiber designs.

Distributed Fiber Raman Amplifier (FRA) using the transmission line as a Raman gain medium is a promising technology available for the long haul

communication systems, especially for Wavelength Division Multiplexing (WDM), where simultaneous amplification of multi-channel lightwave signals is needed, ,as well as for repeaterless transmission, where optical gain is required for compensation of the fiber loss. FRA is to amplify optical signals in optical fibers, based on transferring the power from the pump beam to the signal via Raman interaction between the light and vibrational modes of the glass. Typically, the Raman gain coefficient in fused silica peaks at a Stokes shift of about 13.2 THz with a 3 dB bandwidth of about 6 THz. FRAs exhibit several attractive features for applications in transmission systems, as: i) Simplicity of amplifier architecture, ii) Low noise, iii) Broad gain spectrum, iv) Flexibility of transmission window, and v) Higher saturation power [1,2].

Recent progress in broad-band Raman amplifiers for WDM transmissions was reviewed. The fundamentals of Raman amplifier were discussed in contrast to erbium-doped fiber amplifiers to show excellent applicability of both amplifiers to WDM transmissions in the opposite extremes. A new technique called "WDM pumping" was introduced to obtain sufficient, ultrabroad, and flat gain in Raman amplifiers only using WDM diode pumps. The maximum available Raman gain using this scheme will be increased in accordance with the increasing output power of pump lasers. Then, other limiting factors such as double-Rayleigh-scattering noise may become important. However, the detailed studies in case of WDM pumping based on diode lasers have yet to be conducted [3-5].

A comprehensive analysis of the temperature dependence of a Raman amplifier and the scaling of the Raman gain coefficient with wavelength, modal overlap, and material composition was presented [6]. Also, the temperature dependence was derived by applying a quantum theoretical description, whereas the scaling of the Raman gain coefficient was derived using a classical electromagnetic model. Experimental verification of the theoretical findings was presented also.

A novel numerical method for the standard propagation equations of Raman amplifiers with multiple pumps, was presented and derived based on four-step Adams-Bashforth method [7].

A series of experiments for 128 x 10 GB/s ULH applications and 64 x 40 GB/s ultra-high capacity (UHC) applications based on a common single-wideband platform were discussed: To increase the applicability of their results, fiber dispersion and loss were carried out and chosen to be in accordance with commercially deployed spans. A simple system margins and small transmission penalties were demonstrated on two fiber types true wave reduced slope (TWRS) and standard single mode fiber (SSMF), and validate the feasibility of this approach for deployment in a commercial network. Finally, a simple implementation of an OADM was demonstrated, yielding no observed degradation due to filter-narrowing and/or device dispersion for different sets of multiplexing/de-multiplexing devices [8,9].

160 Gb/s single-channel transmission using a scheme consisting of two super large effective area (SLA) fibers separated by an inverse dispersion fiber (IDF) and Raman amplification had been investigated numerically [10,11]. Backward pumping, bidirectional pumping, and second-order pumping were investigated. For the three schemes, about the same systems the reach of 2500 km was obtained.

An efficient and stable algorithm based on the simple-shooting method to solve the fiber Raman-amplifier equations was proposed and numerically demonstrated

by Q. Han et. al.,[12]. In the algorithm, the conventional Newton-Raphson method was substituted by a more efficient and stable modified Newton method to serve as the correction mechanism in the shooting iterations. By introducing the Broyden's rank-one method into the modified Newton method, the time-consuming calculation of the Jacobian matrix was dramatically relieved, and the efficiency of the proposed algorithm was further remarkably improved. An effective initial-guess providing technique for the shooting method had also been proposed. Simulation results show that the efficiency of the proposed algorithm was improved more than three times compared with those of the previously reported methods. This algorithm can be used in the design of various kinds of FRAs to predict their gain and noise performance accurately [12].

In the present paper, the characteristics of multi-pumping Raman amplifiers employed in ultra-high capacity (UHC) and ultra-long haul (ULH) applications will be deeply and parametrically investigated over wide ranges of affecting causes.

II. BASIC MODE; GOVERNING EQUATIONS, AND ANALYSIS

In the present paper, N_t optical channels are transmitted through N_L optical links for the sake of UHC. Multi-pumping Raman amplifiers are employed via the use of N_R pumps of equal or unequal powers and equal spectral spacing for the sake of ULH. The following characteristics are processed at N_R = {4,6,8,10}: i) The net effective gain constant, G_c, ii) The average effective area, $A_{eff.}$, iii) The average on-off gain, G_{oo}, iv) The average amplified spontaneous emission, ASE, v) The average signal-to-noise ratio, SNR, and finally vi) The average repeater spacing, R_s.

II.1. Numerical data

The following numerical data are employed to obtain the best performance which achieve both UHC and ULH: $1.4 \le \lambda_s, optical\ signal\ wavelength, \mu m \le 1.75$, $1.4 \le \lambda_R, \text{pumping signal wavelength}, \mu\text{m} \le 1.55$, P_R: pumping power = 0.2 Watt/pump, N_R: number of pumps {4,6,8,10}, N_t: total number of channels up to 14400 channels, N_L: total number of links up to 480 links, and $0.004 \le \Delta n$ relative refractive index difference ≤ 0.01

Thus, there is a number of channels per link $N_{ch} = N_t / N_L$, these N_{ch} possess a central wavelength λ_{cL} given by:

$$\lambda_{cL} = \lambda_i + \delta\lambda(N_{oL} - 0.5)N_{ch} \quad , \tag{1}$$

$$\delta\lambda = (\lambda_f - \lambda_i)/(N_t - 1) , \tag{2}$$

with λ_i = 1.4 μm , λ_f = 1.75 μm , and N_{oL} is the order of link {1,2,3,….., N_L}.

II.2. Basic Model

On the same spirit of [13], we have derived the following expression for the solution of the simplified two rates nonlinear-coupled differential equations that describe the propagation of both the signal power P_{si} and the pump power P_{Rj} given under the forms:

$$\frac{dP_{si}}{dL}+\sigma_{si}P_{si}=\left[G_oP_{Rj}+G_1P_{si}\right]P_{si},\ \ \lambda_{si}>\lambda_{Rj}\qquad , \tag{3}$$

$$\frac{dP_{Rj}}{dL}+\sigma_{Rj}P_{Rj}=\left[-G_2P_{si}+G_3P_{Rj}\right]P_{Rj},\ \ \lambda_{si}>\lambda_{Rj}\,, \tag{4}$$

where:

$$G_o=\sum_{j=1}^{N_R}\frac{g_j}{\Gamma A_j}=\frac{g}{\Gamma A}N_{RR},\ \ km^{-1}W^{-1},\ \ \lambda_{si}>\lambda_{Rj}\,, \tag{5}$$

$$G_1=\sum_{j=1}^{i-1}\frac{g_{ij}}{\Gamma A_j}-\sum_{m=i+1}^{N_{ch}}\frac{g_{im}}{\Gamma A_m}.\frac{\lambda_{sm}}{\lambda_{si}},\ \ km^{-1}W^{-1}\,, \tag{6}$$

$$G_2=\sum_{i=1}^{N_{ch}}\frac{g_i}{\Gamma A_i}.\frac{\lambda_{si}}{\lambda_{rj}},\quad km^{-1}W^{-1},\ \ \lambda_{si}>\lambda_{Rj}\,,\text{ and} \tag{7}$$

$$G_3=\sum_{j=1}^{J-1}\frac{g_{jk}}{\Gamma A_j}-\sum_{\ell=J+1}^{N_R}\frac{g_{jk}}{\Gamma A_\ell}.\frac{\lambda_{R\ell}}{\lambda_{RJ}},\ \ km^{-1}W^{-1}\,. \tag{8}$$

N_{RR} is the number of amplifiers of wavelengths λ_{Rj} less than λ_{si}, where $N_{RR}\in\{1,2,3,\ldots\ldots,N_R\}$. The set of coefficients $\{G_o, G_1, G_2, G_3\}$ are recast under the forms: $G_o=N_{RR}G_c\,, G_1=G_c\left[(i-1)-(N_{ch}-i)\lambda_{sa1}/\lambda_{si}\right]=N_1G_c\,,$
$G_2=G_c\left[N_{ch}\lambda_{sa2}/\lambda_{Rj}\right]=N_2G_c\,,$ and $G_3=G_c\left[(J-1)-(N_R-J)\lambda_{Ra}/\lambda_{RJ}\right]=N_3G_c\,.$ with $G_c=<g/\Gamma A>$ the average gain coefficient over a link, $\lambda_{sa1}=(\lambda_{Nch}+\lambda_{i+1})/2\,,$ $\lambda_{sa2}=(\lambda_{s1}+\lambda_{sch})/2,\ \ \lambda_{si}\geq\lambda_{Rj}$

Then, on the same spirit of [13], we assume:

$$P_{si}(L)=U_{si}(L)e^{-\sigma_{si}L},\ \text{ and} \tag{9}$$

$$P_{Rj}(L)=W_{Rj}(L)e^{-\sigma_{Rj}L}\,. \tag{10}$$

Differentiating with respect to L, one gets:

$$\frac{dP_{si}}{dL}=-\sigma_{si}P_{si}+\left(\frac{U_{si}^{\backslash}}{U_{si}}\right)P_{si},\ \text{ and} \tag{11}$$

$$\frac{dP_{Rj}}{dL}=-\sigma_{Rj}P_{Rj}+\left(\frac{W_{Rj}^{\backslash}}{W_{Rj}}\right)P_{Rj}\,. \tag{12}$$

The use of Eqns. (11) and (12) in Eqns. (3) and (4) yields:

$$\left(\frac{U_{si}^{\backslash}}{U_{si}}\right)P_{si}=\left(G_oP_{Rj}+G_1P_{si}\right)P_{si},\ \text{ and} \tag{13}$$

$$\left(\frac{W_{Rj}^{\backslash}}{W_{Rj}}\right)P_{Rj}=\left(-G_2P_{si}+G_3P_{Rj}\right)P_{Rj}\,. \tag{14}$$

For All wave fiber, the assumption $\sigma_{si}=\sigma_{Rj}=\sigma_a$ is good. Thus, Eqns. (13) and (14) give (neglecting here only the interactions G_1 and G_3)

$$\frac{U_{si}^{\backslash}}{U_{si}} = G_o W_{Rj} e^{-\sigma_a L}, \tag{15}$$

$$\frac{W_{Rj}^{\backslash}}{W_{Rj}} = -G_2 U_{si} e^{-\sigma_a L}, \text{ and finally} \tag{16}$$

$$\left(\frac{U_{si}^{\backslash}}{U_{si}}\right).\left(\frac{W_{Rj}}{W_{Rj}^{\backslash}}\right) = \frac{W_{Rj}}{U_{si} G_4}. \tag{17}$$

where: $G_4 = G_2 / G_o = N_2 / N_{RR}$, thus we obtain:

$$N_2 U_{si}^{\backslash} + N_{RR} W_{Rj}^{\backslash} = 0.0. \tag{18}$$

The integration yields:

$$N_{RR} W_{Rj} + N_2 U_{si} = C = N_{RR} P_{Rjo} + N_2 P_{sio} = P_T. \tag{19}$$

C is a constant and is determined from the initial conditions.

The right hand side of Eqn.(19) presents the total injected power at the link entrance (L=0.0). From Eqn.(19), we have:

$$W_{Rj} = (P_T - N_2 U_{si}) / N_{RR} \tag{20}$$

The use of Eqn.(20) into Eqn.(13) yields:

$$\frac{U_{si}^{\backslash}}{U_{si}} = \left[G_c (P_T - N_2 U_{si}) / N_{RR} + G_1 U_{si}\right] e^{-\sigma_a L}, \text{ or}$$

$$\frac{U_{si}^{\backslash}}{U_{si}} - \frac{U_{si}^{\backslash}}{U_{si} + G_5 / G_6} = G_5 e^{-\sigma_a L} \tag{21}$$

Then, the integration yields:

$$\frac{G7}{U_{si}} + 1 = \left(\frac{G_7}{Uso} + 1\right)\left(e^{-G_5 (1 - e^{-\sigma_a L}) / \sigma_a}\right), \tag{22}$$

where: $G_5 = G_c P_T$, $G_6 = (G_1 - G_c N_2)$, and $G_7 = G_5 / G_6$.

Finally, we obtain:

$$P_{si}(L) = \frac{G_7 e^{-\sigma_{si} L}}{\left(\frac{G_7}{U_{so}} + 1\right)\left(e^{-G_5 (1 - e^{-\sigma_a L}) / \sigma_a}\right) - P_{sio}}. \tag{23}$$

In Eqn.(23), we have: $G_6 G_7 = P_T G_c$, km^{-1}, and $L_{eff} = \left(1 - e^{-\sigma_a L}\right) / \sigma_a$, km, thus

$$P_{si}(L) = \frac{P_{sio} G_7 e^{-\sigma_{si} L}}{\left(P_{sio} + G_7\right)\left(e^{-P_T G_c L_{eff}}\right) - 1} = G_T(L) P_{sio} e^{-\sigma_{si} L}, \tag{24}$$

where: $G_T(L) = G_7\left(\left(P_{sio} + G_7\right) e^{-P_T G_c L_{eff}} - P_{sio}\right)^{-1}$ is a dimensionless variable.

In the above equations $P_{si}(L)$, G_c, P_{Rjo}, P_{sio}, L_{eff}, σ_{si} are respectively signal power at a distance L, effective total Raman gain coefficient, Raman pump power at L=0.0, signal power at L=0.0, effective length, and the spectral losses in km^{-1}. G_c is given by:

$$G_c(\lambda_{cL}, \lambda_{RA}, g_o) = g(\lambda_{cL}, \lambda_{RA}) / \left[\Gamma A_e(\lambda_{cL}, \lambda_{RA})\right] \tag{25}$$

where $g(\lambda_{cL}, \lambda_{RA})$ and $A_e(\lambda_{cL}, \lambda_{RA})$ are functions of both the central wavelength and the average Raman pumps wavelengths, and $\Gamma = 2$ for the polarization effect.

In the first part of the present paper, G_c, A_e, and ASE are computed and cast in simple polynomial forms, with very small truncation errors and very small relative RMS errors as:

$$G_c = \sum_{i=0}^{3} A_i \lambda_{cL}^i \quad (\text{with} \quad A_i = \sum_{j=0}^{3} a_{ji} \Delta^j), \tag{26}$$

$$A_e = \sum_{i=0}^{3} B_i \lambda_{cL}^i \quad (\text{with} \quad B_i = \sum_{j=0}^{3} b_{ji} \Delta^j), \tag{27}$$

$$ASE = \sum_{i=0}^{3} C_i \lambda_{cL}^i \quad (\text{with} \quad C_i = \sum_{j=0}^{3} c_{ji} \Delta^j), \tag{28}$$

with: $\lambda_{cL} > \lambda_{RA}$ to obtain amplification.

The above quantities are handled at $N_R \in \{4,6,8,10\}$ with relative small RMS errors, where,

$$\begin{bmatrix} A_0 \\ A_1 \\ A_2 \\ A_3 \end{bmatrix} = \begin{bmatrix} a_{00} & a_{10} & a_{20} & a_{30} \\ a_{01} & a_{11} & a_{21} & a_{31} \\ a_{02} & a_{12} & a_{22} & a_{32} \\ a_{03} & a_{13} & a_{23} & a_{33} \end{bmatrix} \begin{bmatrix} 1 \\ \Delta \\ \Delta^2 \\ \Delta^3 \end{bmatrix}, \tag{29}$$

$$\begin{bmatrix} B_0 \\ B_1 \\ B_2 \\ B_3 \end{bmatrix} = \begin{bmatrix} b_{00} & b_{10} & b_{20} & b_{30} \\ b_{01} & b_{11} & b_{21} & b_{31} \\ b_{02} & b_{12} & b_{22} & b_{32} \\ b_{03} & b_{13} & b_{23} & b_{33} \end{bmatrix} \begin{bmatrix} 1 \\ \Delta \\ \Delta^2 \\ \Delta^3 \end{bmatrix}, \tag{30}$$

$$\begin{bmatrix} C_0 \\ C_1 \\ C_2 \\ C_3 \end{bmatrix} = \begin{bmatrix} c_{00} & c_{10} & c_{20} & c_{30} \\ c_{01} & c_{11} & c_{21} & c_{31} \\ c_{02} & c_{12} & c_{22} & c_{32} \\ c_{03} & c_{13} & c_{23} & c_{33} \end{bmatrix} \begin{bmatrix} 1 \\ \Delta \\ \Delta^2 \\ \Delta^3 \end{bmatrix}, \tag{31}$$

where $1.4 \le \lambda_{cL}, \mu m \le 1.75$, $1.4 \le \lambda_R, \mu m \le 1.55$, and $0.004 \le \Delta \le 0.01$.

The net effective gain $G_c(\lambda_{cL}, \lambda_{RA})$, and both $g(\lambda_{si}, \lambda_{RA})$ and $A_e(\lambda_{si}, \lambda_{RA})$ are computed based on the data of each link N_{oL} where $\lambda_{1L} \le \lambda_{si} \le \lambda_{2L}$ and

$$\lambda_{1L} = \lambda_i + \delta\lambda(N_{oL} - 1)N_{ch}, \tag{32}$$

$$\lambda_{2L} = \lambda_{1L} + \delta\lambda N_{ch} = \lambda_i + N_{oL} N_{ch}, \tag{33}$$

$$\lambda_{si} = \lambda_{1L} + \delta\lambda(I - 1)N_{ch}, \tag{34}$$

with i = {1,2,3,….., N_{ch}}.

Then, both $g(\lambda_{si}, \lambda_{RA})$ and $A_e(\lambda_{si}, \lambda_{RA})$ are averaged to give:

$$g(\lambda_{cL}, \lambda_{RA}) = \frac{1}{N_{ch}} \sum_{i=1}^{N_{ch}} g(\lambda_{si}, \lambda_{RA}), \text{ and} \tag{35}$$

$$A_e(\lambda_{cL}, \lambda_{RA}) = \frac{1}{N_{ch}} \sum_{i=1}^{N_{ch}} A_e(\lambda_{si}, \lambda_{RA}). \tag{36}$$

In such a manner, we obtain both $A_e(\lambda_{cL},\lambda_{RA})$ and $g(\lambda_{cL},\lambda_{RA})$ and consequently we cast $G_c(\lambda_{cL},\lambda_{RA})$. Based on the model of [13], $ASE(\lambda_{cL},\lambda_{RA})$, as a criterion of the minimum detectable power, is computed. The signal light must be amplified again before its level becomes less than that of the ASE. In order to obtain the ASE power at the output end of the fiber for signal power amplification, the idea of effective input Stokes power $P_{s\text{-}eff}$ as the ASE is employed:

$$P_{s-eff} = h\nu B_{eff} \quad \text{, where} \tag{37}$$

$$B_{eff} = \left(\sqrt{\pi}/2\right)\left(\Delta\nu_{FWHM}/\left(P_{Rj}G_c/\sigma_{Rj}\right)^{0.5}\right), \tag{38}$$

where h is Planck's constant and $\Delta\nu_{FWHM}$ is assumed as the full width at half-maximum of gain profile. The actual Raman gain profile is very wide, and $P_{s\text{-}eff}$ is large, $\Delta\nu_{FWHM}$ of 300 GHz is used in the following study. Finally from Eqns.(37) and (38), ASE power in Watt is given by:

$$ASE = \left(2.981326x10^{-8}/\lambda_s\right)\sqrt{\left(\pi\sigma_{Rj}/4.343\right)/P_{Rjo}G_c} \tag{39}$$

The average repeater spacing in link of order N_{oL}., $R_{SA}(N_{oL})$ is given by:

$$R_{SA}(N_{oL}) = \frac{1}{N_{ch}}\sum_{i=1}^{N_{ch}} R_{si}\,, \tag{40}$$

where R_{si} satisfies:

$$P_{si}(R_{si}) = G_T(R_{si})P_{sio}e^{-\sigma_{si}R_{si}} = ASE(\lambda_{si},\lambda_{RA}) \tag{41}$$

with $L_{eff} = \left(1-e^{-\sigma_a R_{si}}\right)/\sigma_a$, km.

The average Raman on-off gain G_{oo} per link and the average SNR per link are given are defined as:

$$G_{oo} = \frac{1}{N_{ch}}\sum_{i=1}^{N_{ch}} 10Log_{10}\left[P_{si}(L,P_R)/P_{si}(L,0)\right], \text{ and} \tag{42}$$

$$SNR = \frac{1}{N_{ch}}\sum_{i=1}^{N_{ch}} 10Log_{10}\left(P_{si}(L,P_R)/ASE\right). \tag{43}$$

In the present study, we have considered $L = L_{eff} = 1.5/\sigma_{si}$, km, in Eqns. (42) and (43). A special algorithm is designed to process the present paper parametrically over the numerical data given in part II.2. Based on the data published [3,6,7,14-18], listed in Table I, we processed our model, taking the theoretical limit of the repeater spacing which was given by [19].

Table I :Data processed for {4,6,8} as samples of multi-pumping Raman Amplifier

P_R , W [14]	λ_R, μm (N_R = 4)
0.4	1.42
0.35	1.4355
0.15	1.4515
0.17	1.480
$\sum P_R = 1.07$	

P_R , W [6]	λ_R, μm (N_R = 4)
0.265	1.4236
0.265	1.4438
0.265	1.47103
0.265	1.496
$\sum P_R = 1.061$	

P_R , W [16]	λ_R, μm (N_R = 6)
0.28892	1.44127
0.30696	1.44823
0.12264	1.47056
0.150	1.4720
0.18255	1.47602
0.1629	1.48994
$\sum P_R = 1.21397$	

P_R , W [17]	λ_R, μm (N_R = 6)
0.2942	1.4152
0.2816	1.4274
0.1335	1.444
0.1523	1.4585
0.1242	1.473
0.14107	1.5092
$\sum P_R = 1.12687$	

P_R , W [17]	λ_R, μm (N_R = 6)
0.2999	1.4152
0.1715	1.4274
0.0633	1.444
0.0783	1.4585
0.0717	1.473
0.0619	1.5092
$\sum P_R = 0.7466$	

P_R , W [18]	λ_R, μm (N_R = 8)
0.0826	1.4504
0.0826	1.4579
0.0826	1.465
0.0826	1.4731
0.0826	1.4808
0.0826	1.4886
0.0826	1.4958
0.0826	1.5028
$\sum P_R = 0.6608$	

P_R , W [7]	λ_R, μm (N_R = 8)
0.063	1.415
0.056	1.420
0.050	1.424
0.043	1.429
0.043	1.440
0.043	1.457
0.048	1.4748
0.063	1.502
$\sum P_R = 0.409$	

P_R , W [3]	λ_R, μm (N_R = 8)
0.09	1.426
0.095	1.428
0.070	1.444
0.09	1.454
0.07	1.462
0.080	1.465
0.190	1.492
0.176	1.493
$\sum P_R = 0.861$	

The present investigation

P_R , W	λ_R, μm (N_R = 4)
0.24	1.4
0.24	1.4333333
0.24	1.4666666
0.24	1.5
$\sum P_R = 0.96$ W	

P_R , W	λ_R, μm (N_R = 6)
0.16	1.4
0.16	1.42
0.16	1.44
0.16	1.46
0.16	1.48
0.16	1.5
$\sum P_R = 0.96$ W	

P_R , W	λ_R, μm (N_R = 8)
0.12	1.4
0.12	1.4142857
0.12	1.4285714
0.12	1.4428571
0.12	1.4571428
0.12	1.4714285
0.12	1.4857142
0.12	1.5
$\sum P_R$ = 0.96 W	

P_R , W	λ_R, μm (N_R = 10)
00.96	1.4
0.096	1.4111111
0.096	1.4222222
0.096	1.4333333
0.096	1.4444444
0.096	1.4555555
0.096	1.4666666
0.096	1.4777777
0.096	1.4888888
0.096	1.5
$\sum P_R$ = 0.96 W	

III. RESULTS AND DISCUSSION

III.1. Introduction

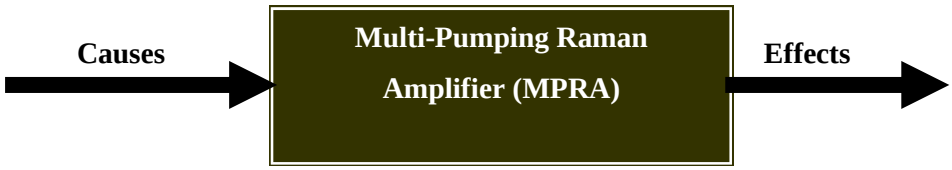

Fig.1. Causes and Effects in MPRA

In the present paper both the causes and the resulted effects are as follows: i) Causes are N_t, N_L, $N_{oL}(\lambda_{cL})$, N_{ch}, Δn, N_R, P_{sio}, P_{Rjo}, and P_{RT}, where the set of major interest is $\{N_t, N_L, N_R, P_{RT}\}$, and ii) Effects are G_c, A_e, G_{oo}, ASE, SNR, R_s (maximum theoretical limit) [19]. The given effects are investigated at the propagation distances: R_s which equals to $1.5/\sigma_{si}$ which is considered as L_{eff}. Based on the reported data [20], we employed AllWave fiber of spectral losses $\sigma_s(\lambda_s)$, where we have cast:

$$\sigma_{sd}(\lambda_s) = 0.19319 + 6.234\lambda_m^2 + 27.902\lambda_m^3 - 9.1542\lambda_m^4 - 341.85\lambda_m^5 - 525.81\lambda_m^6 \ \text{dB/km},$$

where $\lambda_m = \lambda_s - 1.55$, and $\sigma_{sk}(\lambda_s) = \sigma_{sd}(\lambda_s)/4.343 \ \text{km}^{-1}$

Variations of the set of effects $\{G_c, A_e, G_{oo}, ASE, SNR, R_s\}$ against variations of the subset of causes $\{\Delta, N_R, N_{oL}(\lambda_{cL})\}$ are depicted in Figs. 2-17 and will be discussed in the following subsections.

III.2. Variations of Average Repeater Spacing, R_s

These variations against N_L as a major cause are clarified in Figs.2-7 at two levels of the total channels N_T = {7200, 14400}, at three levels of amplification N_R = {4,6,8}, and at three different refractive index differences Δn = {0.005,0.0075,0.01}. The above figures indicate the following: i) R_s and any subset of the set of causes $\{N_L, P_{RT}, \Delta n\}$ are in positive correlations, ii) R_s and N_T are in negative correlations, and iii) The total injected Raman powers are the vital factor rather than the number of amplifier, where it

is clear that: $P_{RT}(N_R = 4) = 1.06 \rightarrow 1.07$ W , $P_{RT}(N_R = 6) = 0.74 \rightarrow 1.214$ W , and $P_{RT}(N_R = 8) = 0.409 \rightarrow 0.861$ W .

N_T = 7200 channels, Fig.2		N_T = 14400 channels, Fig.3
N_R= 4,6,8 1.45 < λ, μm < 1.65, P_S=0.2 mW Δn=0.0075, $P_{RT}(N_R = 4)$ = 1.07 Watt , $P_{RT}(N_R = 6)$ = 1.3965 Watt, $P_{RT}(N_R = 8)$ = 0.409 Watt		

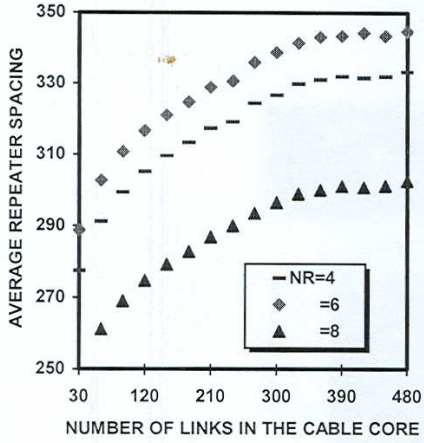

Fig.2. Variations of average repeater spacing, R_s, km with number of links in the cable core, N_L, at the assumed set of parameters.

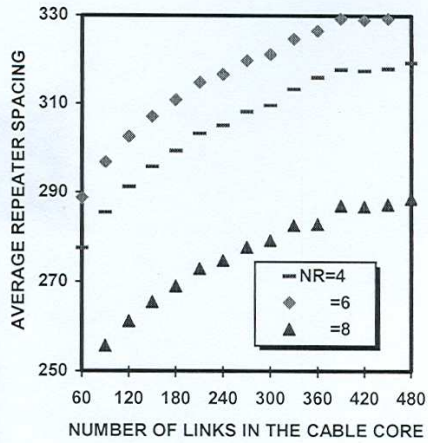

Fig.3. Variations of average repeater spacing, R_s, km with number of links in the cable core, N_L, at the assumed set of parameters.

N_T =7200 channels, Fig.4		N_T = 14400 channels, Fig.5
N_R= 4 $P_{RT}(N_R = 4)$ = 1.07 Watt 1.45 < λ, μm < 1.65, P_S=0.2 mW		

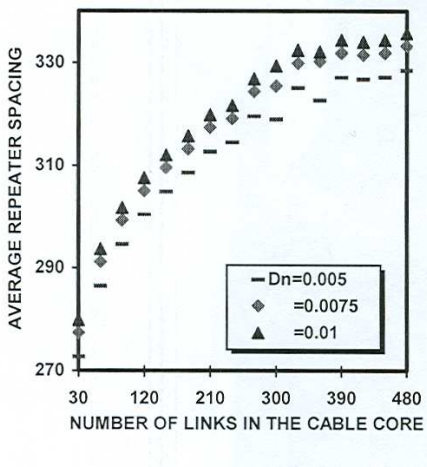

Fig.4. Variations of average repeater spacing, R_s, km with number of links in the cable core, N_L , at the assumed set of parameters.

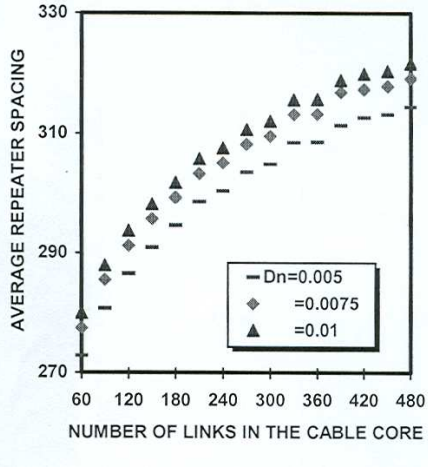

Fig.5. Variations of average repeater spacing, R_s, km with number of links in the cable core, N_L, at the assumed set of parameters.

N_T =7200 channels, Fig.6		N_T = 14400 channels, Fig.7
N_R= 8 $P_{RT}(N_R = 8)$ = 0.409 Watt 1.45 < λ, μm < 1.65, P_S=0.2 mW		

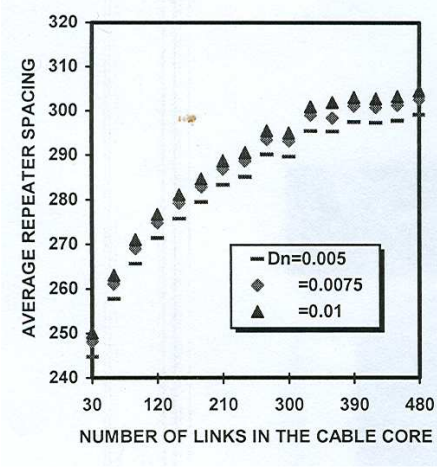

Fig.6. Variations of average repeater spacing, R_s, km with number of links in the cable core, N_L , at the assumed set of parameters.

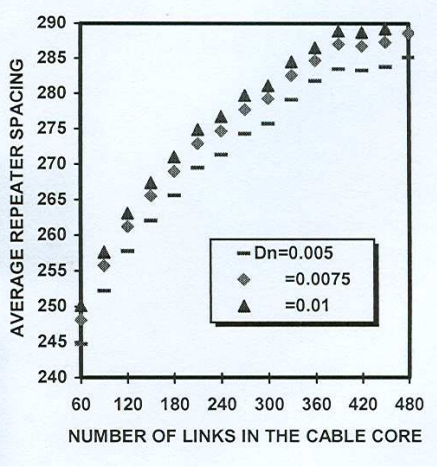

Fig.7. Variations of average repeater spacing, R_s, km with number of links in the cable core, N_L , at the assumed set of parameters.

III.2. Variations of G_c, and G_{oo}

Variation of Raman gain constant, G_c and variations of the on-off Raman gain, G_{oo} against N_L as a major cause are portrayed in Figs.8-13 at the effective length. These figures assure the sort of variations of R_s whatever the controlling sets of causes.

N_T =7200 channels, Fig.8		N_T = 14400 channels, Fig.9
N_R= 4,6,8 1.45 < λ, μm < 1.65, P_S=0.2 mW Δn=0.0075, $P_{RT}(N_R = 4)$ = 1.07 Watt , $P_{RT}(N_R = 6)$ = 1.3965 Watt, $P_{RT}(N_R = 8)$ = 0.409 Watt		

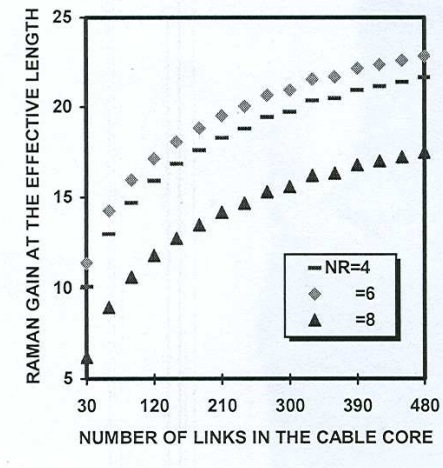

Fig.8. Variations of Raman gain at the effective length, dB with number of links in the cable core, N_L, at the assumed set of parameters.

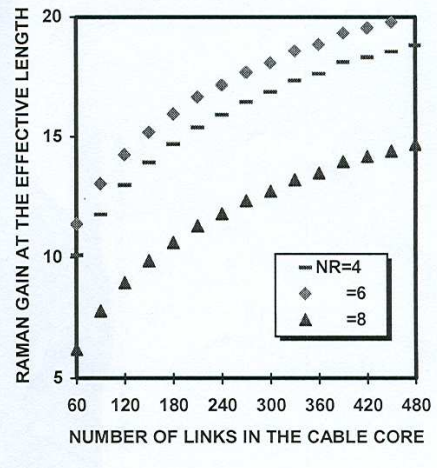

Fig.9. Variations of Raman gain at the effective length, dB with number of links in the cable core, N_L , at the assumed set of parameters

N_T =7200 channels, Fig.10		N_T = 14400 channels, Fig.11
N_R= 4,6,8 1.45 < λ, μm < 1.65, P_S=0.2 mW Δn=0.0075,		
$P_{RT}(N_R = 4)$ = 1.07 Watt , $P_{RT}(N_R = 6)$ = 1.3965 Watt, $P_{RT}(N_R = 8)$ = 0.409 Watt		

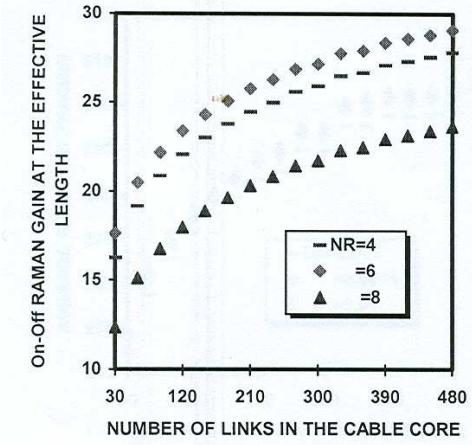

Fig.10. Variations of On-Off Raman gain at the effective length, G_{On-Off}, dB with number of links in the cable core, N_L , at the assumed set of parameters.

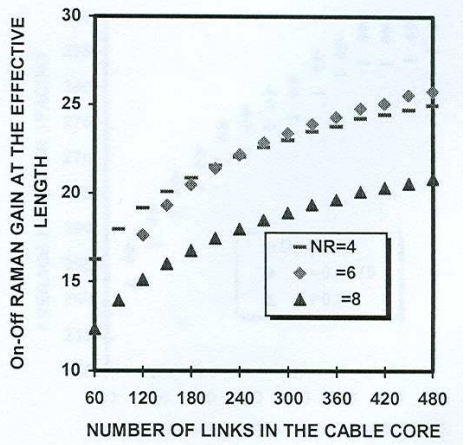

Fig.11 Variations of On-Off Raman gain at the effective length, G_{On-Off}, dB with number of links in the cable core, N_L, at the assumed set of parameters

N_T =7200 channels, Fig.12		N_T = 14400 channels, Fig.13
N_R= 4,6,8 1.45 < λ, μm < 1.65, P_S=0.2 mW Δn=0.0075,		
$P_{RT}(N_R = 4)$ = 1.07 Watt , $P_{RT}(N_R = 6)$ = 1.3965 Watt, $P_{RT}(N_R = 8)$ = 0.409 Watt		

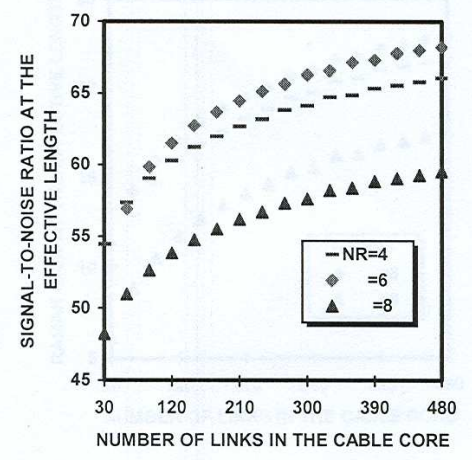

Fig.12. Variations of signal-to-noise ratio at the effective length with number of links in the cable core, N_L, at the assumed set of parameters.

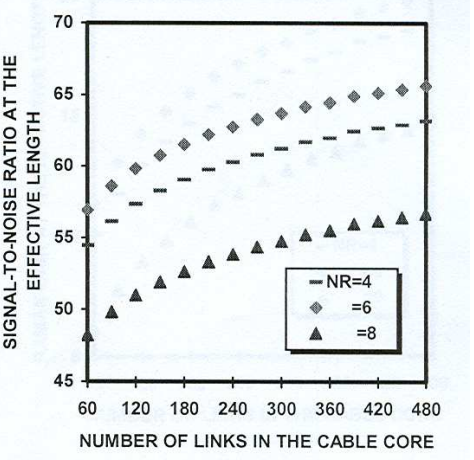

Fig.13 Variations of signal-to-noise ratio at the effective length with number of links in the cable core, N_L , at the assumed set of parameters

III.3. Variations of SNR

Variations of signal-to-noise S/N, also at the effective length are displayed in Figs.14-17 where the following are clarified: i) S/N increases as N_L increases, or Δn increases, or N_{ch} decreases or both, and ii) The total Raman injected power P_{RT} possesses remarkable effect also on the ratio S/N.

N_T =7200 channels, Fig.14		N_T = 14400 channels, Fig15
N_R= 4 1.45 < λ, μm < 1.65, P_S=0.2 Mw		$P_{RT}(N_R = 4)$ = 1.07 Watt

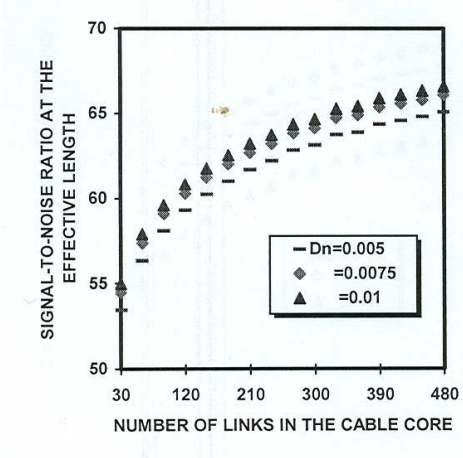

Fig.14. Variations of signal-to-noise ratio at the effective length with number of links in the cable core, N_L, at the assumed set of parameters.

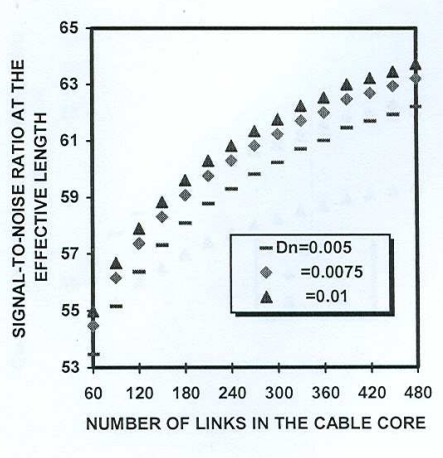

Fig.15 Variations of signal-to-noise ratio at the effective length with number of links in the cable core, N_L, at the assumed set of parameters

N_T =7200 channels, Fig.16		N_T = 14400 channels, Fig.17
N_R= 8 1.45 < λ, μm < 1.65, P_S=0.2 mW		$P_{RT}(N_R = 8)$ = 0.409 Watt

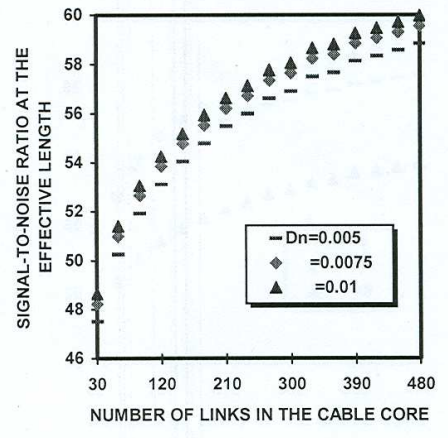

Fig.16. Variations of signal-to-noise ratio at the effective length with number of links in the cable core, N_L, at the assumed set of parameters.

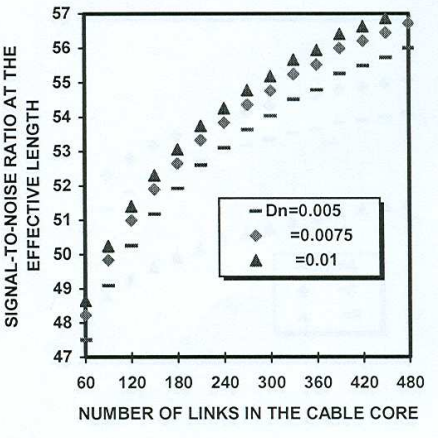

Fig.17 Variations of signal-to-noise ratio at the effective length with number of links in the cable core, N_L, at the assumed set of parameters

III.4. Case of Constant Pumping Power and Multi-Pump

At the effective length, variations of average repeater spacing R_s, average Raman gain, and average on-off Raman gain against number of links are clarified in Figs.18-20, where number of pumps are variable, while the total pumping power is constant. Again, these results assure that the total pumping power is a vital factor, not the number of pumps.

N_T =14400 channels	N_R= 4,6,8, 10	1.45 < λ, μm < 1.65
P_S=0.2 mW	Δn=0.0075, P_{RT} = 0.96 Watt	1.4 < λ_R μm < 1.5

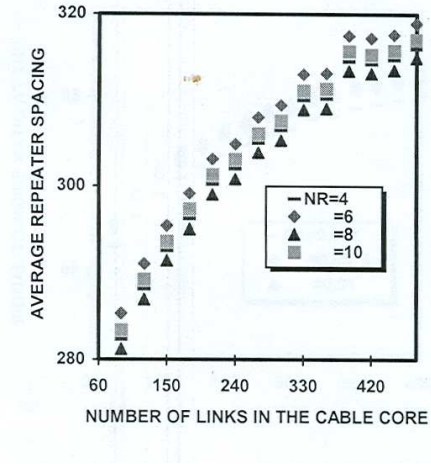

Fig.18. Variations of average repeater spacing, R_s, km with number of links in the cable core, N_L, at the assumed set of parameters.

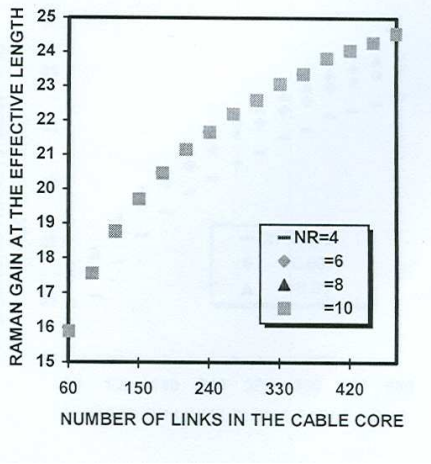

Fig.19. Variations of average Raman gain, dB with number of links in the cable core, N_L , at the assumed set of parameters.

N_T =14400 channels	N_R= 4,6,8, 10	1.45 < λ, μm < 1.65
P_S=0.2 mW	Δn=0.0075, P_{RT} = 0.96 Watt	1.4 < λ_R μm < 1.5

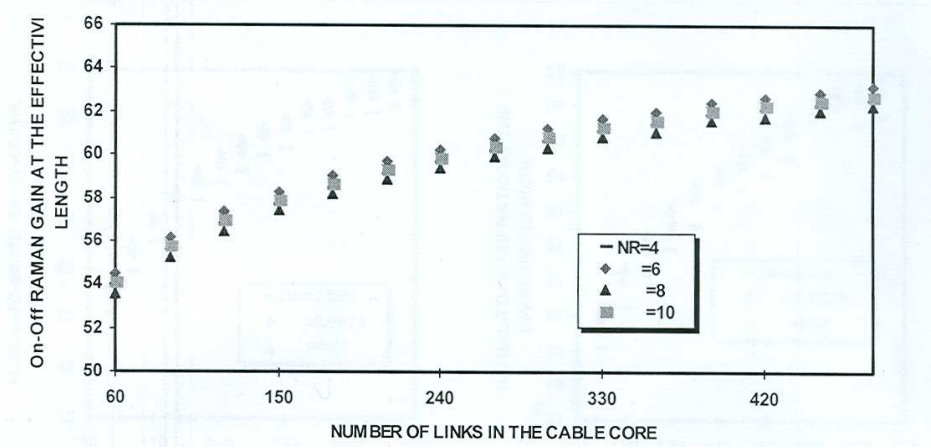

Fig.20. Variations of On-Off Raman gain at the effective length, $G_{On\text{-}Off}$, dB with number of links in the cable core, N_L, at the assumed set of parameters.

IV. CONCLUSIONS

In the present paper, the net effective gain of multi-pumping Raman amplifier in ultra-wavelength division multiplexing (WDM) and ultra long-haul optical communication systems has been modeled and parametrically investigated over wide ranges of affecting parameters, taking into account the polarization effect.

Repeater spacing, R_s, net Raman gain, G_c , on-off Raman gain, G_{oo}, and signal-to-noise ratio, SNR, effects are as major parametrically investigated under variations of major sets of causes employing multi-pumping Raman amplifier (MPRA) at different pumping conditions. The investigation indicates the following integrated conclusions: i) Both the total number of links in the core N_L and the total Raman injected power of pumps (not the number of pumps) P_{RT} are causes of vital effects, ii) R_s, G_c, G_{oo}, SNR, and ASE (not displayed), as a criterion to account the minimum detectable power, and any subset of the following set $\{N_L, P_{RT}, \Delta n, N_{ch}\}$ are in positive correlations, iii) SNR and either N_R or N_{ch} or both are in negative correlations.

REFERENCES

[1] A.S. Jazi, Calculations and Measurements of Raman Gain Coefficients of Different Fiber Types, M.Sc. Thesis in Electrical Engineering, Fac. Virginia Polytechnic Institute, USA, Dec., **2002.**

[2] C. Headley and G.P. Agrawal, Raman Amplification in Fiber Optical Communication Systems, Elsevier AP, USA, **2005**

[3] S. Namiki and Y. Emorg, "Ultrabroad-Band Raman Amplifiers Pumped and Gain-Equalized by Wavelength-Division-Multiplexed High-Power Laser Diodes," IEEE J. Selected Topics in Quantum Electronics, Vol.7, No.1, pp. 3-16, Jan./Feb.**2001**.

[4] V.E. Perlin and H.G. Winful, "On Distributed Raman Amplification for Ultrabroad-Band Long-Haul WDM Systems," J. Lightwave Technol., Vol.20, No.3, pp.409-416, March **2002**.

[5] M.N. Islam, "Raman Amplifiers for Telecommunications," IEEE J. Selected Topics Quantum Electron., Vol. 8, pp.548-559, May/June **2002**.

[6] K. Rottwitt, J.Bromage, A.J. Stentz, L. Leng, M.E. Lines, and H. Smith, "Scaling of the Raman Gain Coefficient: Applications to Germanosilicate Fibers," J. Lightwave Technol., Vol.21, No.7, pp.1652-1662, July, **2003**.

[7] X. Lin, H. Zhang, and Y. Guo, "A Novel Method for Raman Amplifier Propagation Equations," IEEE Photonics Lett., Vol. 15, No.3, pp.392-394, March **2003.**

[8] S. Banerjee, A. Agrwal, D. Grosz, A. Kung, D. Maywar, M. Movas Saght, and T.H. Wood, "Long-Haul 64x40 Gb/s DWDM Transmission Over Commercial Fiber Types with Large Operating Margins," Electron., Lett., Vol.39, p.92, **2003**.

[9] D.F. Grosz, A. Agarwal, S. Banerjee, D.N. Maywar, A.P. Kung, "All-Raman Ultra-Long-Haul Single-Wideband DWDM Transmission Systems with OADM Capability," J. Lightwave Technol., Vol.22, No.2, pp.423-432, Feb. **2004**.

[10] Z. Xu, K Roltwitt, C. Peucheret, and D. Jeppesen, "Optimization of Pumping Schemes for 160 Gb/s Single-Channel Raman Amplified Systems, " IEEE Photonics Technol. Lett., Vol.16, No.1, pp.329-331, Jan. **2004**.

[11] B. Cuenot, "Comparison of Engineering Scenarios for N x 160 Gb/s WDM Transmission Systems," IEEE Photon. Technol. Lett., Vol.15, pp.864-866, June **2002.**

[12] Q. Han, J. Ning, H. Zhang, and Z. Chen, "Novel Shooting Algorithm for Highly Efficient Analysis of Fiber Raman Amplifiers," J. Lightwave Technol., Vol.24, No.4, p.4946, April **2006**.

[13] M.S. Kao and J. Wu, "Signal Light Amplification by Stimulated Raman Scattering in an N-Channel WDM Optical Communication Systems," J. Lightwave Technol., Vol.7, No.9, pp.1290-1299, Sep. **1989**.

[14] S.M. Kobtsev and A.A. Pustovskikh, "Improvement of Raman Gain Flatness by Broadband Pumping Sources," Laser Physics, Vol. 14, No.12, pp.1488-1491, **2004**

[15] L.X_Ming and L. Y_He, "Optimal Bandwidth for Distributed Multi-Pumping Raman Amplifier Based on Hybrid Genetic Algorithm," China Phys. Lett., Vol. 21, No.1, pp. 84-86, **2004**.

[16] J. Chen, X. Liu, Lu, Y. Wang, and Z. Li, "Design of Multi-Stage Gain-Flattened Fiber Raman Amplifiers," J. Lightwave Technol., Vol.24, No.2, pp.935-944, Feb. **2006**.

[17] N. Kikuchi et.al., "Novel In-Service Wavelength-Based Upgrade Scheme for Fiber Raman Amplifier," IEEE Photonics Technol. Lett. Vol. 15, No. 1, pp. 27-29, Jan. **2003**.

[18] X. Liu and B. Lee," A Fast and Stable Method for Raman Amplifier Propagation Equations," Optics Express, Vol. 11, No.18, pp. 2163-2176, Aug. **2003**.

[19] T. Nakashima, S. Seikai, M. Nakazawa, and Y. Negishi, "Theoretical Limit of Repeater Spacing in an Optical Transmission Line Utilizing Raman Amplification," J. Lightwave Technol., Vol..LT-4, No.8, pp.1267-1272, Aug. **1986**.

[20] W. H. Knox, "The Future of WDM, "OPN Trends, pp.5-6, March 2001.

الكسب الصافي الفعال لمكبر "رامان" متعدد الضخ في نظم الاتصالات البصرية فائقة الامتداد وفائقة مضاعفة الإرسال بتعدد الأطوال الموجية

في هذا البحث تم عمل نموذج حاكم ودراسة بارا مترية عميقة على مدى واسع من البارامترات المؤثرة للكسب الصافي الفعال لمكبر "رامان" متعدد الضخ في نظم الاتصالات البصرية فائقة الامتداد وفائقة مضاعفة الإرسال بتعدد الأطوال الموحية.
هذا وقد أخذ في الاعتبار أثر الاستقطاب حيث تم معالجة N_R من المضخات مع التحكم في الفوارق الطيفية. تم دراسة ثلاثة كميات هامة هي: مساحة مقطع الليف الفعالة Effective Core area ، معاملات الكسب (Gain Coefficients)، وأصغر قدرة انبعاث (Amplified Spontaneous Emission, ASE) كمقياس للحد الأدنى للقدرة عند الكاشف (Detector)) على مدى الطول الموحى تحت الاختبار. حيث تم وضع هذه الكميات في صورة كثيرات حدود ، هذا وقد تم معالجة متوسط الكميات التالية: معامل الكسب (Gain Coefficient, G_c) ، معامل كسب الفتح والغلق (On-Off Gain, G_{on-off}) ، ونسبة قدرة الإشارة إلى قدرة الضوضاء (Signal-to-Noise Ratio, S/N) كل ذلك عند الطول الفعال (Effective Length, L_{eff}) . استخدمت النتائج التي تم الحصول عليها لإيجاد متوسط المسافات البينية بين المعيدات (Average Repeater Spacing, R_s)
هذا وقد تم استنتاج أن قدرات الضخ الكلية هي العامل المصيري أكثر من عدد المضخات وذلك عند حساب المسافات البينية ولكن عند حساب عرض النطاق فان عدد المضخات هو العامل المصيري.
هذا وقد أوضحت النتائج إن عدد الوصلات الليفية (Links in a Core) في الكابل بالإضافة إلى مجموع قوى الضخ (Total Pumping Powers) هي المسببات المصيرية (الفعالة) ، حيث ترتبط الكميات (R_s, G_c, G_{on-off}, ASE) مع المسببات (N_L, $N_{ch/Link}$, P_{RT}, Δn) ارتباطا موجبا بينما ترتبط الكمية S/N ارتباطا سالبا مع N_R (عدد المضخات).